

# Reversion of Alignment Direction in the Thermally Enhanced Photoorientation of Photo-Cross-Linkable Polymer Liquid Crystal Films

Nobuhiro Kawatsuki,\* Kohei Goto, Tetsuro Kawakami, and Tohei Yamamoto

Department of Applied Chemistry, Himeji Institute of Technology,  
2167 Shosha Himeji, 671-2201 Japan

Received August 10, 2001; Revised Manuscript Received October 30, 2001

**ABSTRACT:** Reversion of the in-plane reorientation direction of mesogenic groups has been observed for the first time in novel polymethacrylate liquid crystal (PLC) films substituted with a 4-methoxycinnamoyloxybiphenyl side group. The reversion was generated by irradiation with linearly polarized ultraviolet (LPUV) light and a subsequent annealing. Irradiation with LPUV light induces negative optical anisotropy of the films as a result of an axis-selective photoreaction of the side groups. The direction of the thermally enhanced reorientation is dependent on the degree of photoreaction and the distribution of photoproducts, while the induced orientational order in both directions,  $S$ , was larger than 0.5. The distribution of photoproducts in PLC films has been analyzed to elucidate their contribution to the thermally enhanced reorientation behavior. Initially upon photoreaction, thermal enhancement of the photoinduced negative optical anisotropy was observed. However, when the degree of photodimerization was 15% or greater, the direction of the thermally enhanced reorientation was found to be parallel to the polarization direction ( $\mathbf{E}$ ) of LPUV light. It is concluded that a small amount of photoproduct plays a role in the thermal amplification of the photoinduced negative optical anisotropy in a manner identical to that of PLC with azobenzene side groups. In contrast, photodimerized mesogenic groups generated reversion of the orientational direction and enhancement of positive optical anisotropy of the film through annealing.

## 1. Introduction

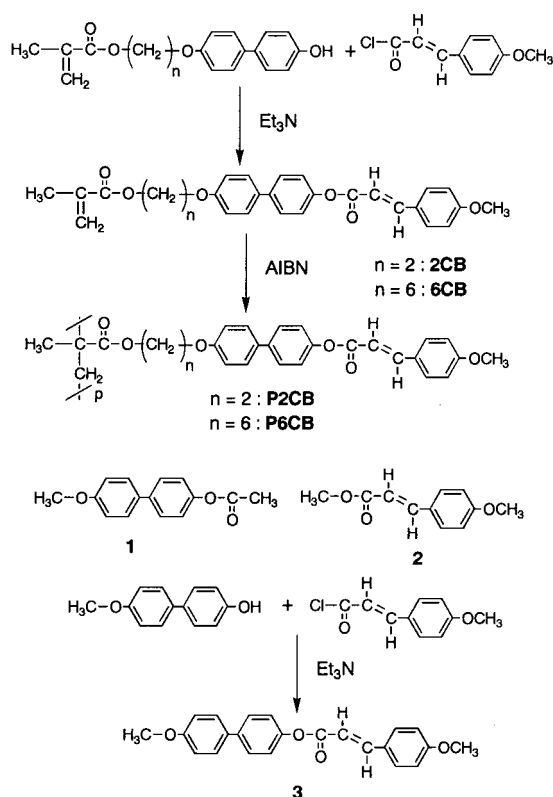
The controlled alignment of molecules in photoreactive polymer films induced by photoirradiation generates unusual birefringent characteristics which may prove to be useful in various kinds of optical devices, such as optical memory devices, holographic elements, and phase retarders for liquid crystal displays.<sup>1–6</sup> Several types of materials have been reported, including azobenzene-containing polymers and photo-cross-linkable polymers, which can generate optical anisotropy of their films upon irradiation with linearly polarized (LP) light.<sup>7–22</sup> In particular, numerous studies of azobenzene-containing polymers have been performed to characterize the axis-selective  $E$ -to- $Z$  photoisomerization reaction which leads to in-plane, high molecular reorientation in a direction perpendicular to the electric vector ( $\mathbf{E}$ ) of LP light.<sup>7–15</sup> Alternatively, we studied a photo-cross-linkable polymer liquid crystal (PLC) containing a cinnamoyloxyethoxybiphenyl side group and its copolymers which exhibit thermally stable reorientation of mesogenic side groups by the use of LP ultraviolet (LPUV) light and subsequent annealing.<sup>20–22</sup> The photo-cross-linked mesogenic groups were found to realign in the direction parallel to  $\mathbf{E}$  of LPUV light, caused by the axis-selective photoreaction of the cinnamoyl substituent.<sup>21</sup> However, the influence of the photoisomerization of the cinnamoyl group has not been elucidated due to the difficulty of spectrum analysis for such a mesogenic group. This system demonstrates three-dimensional orientation of the film by slantwise LPUV exposure, no absorption in the visible region, and high thermal stability;<sup>23</sup> however, the induced reorientational order of the films is low compared to that of azobenzene-containing PLCs.

If the in-plane orientation can be controlled both parallel and perpendicular to  $\mathbf{E}$  of LP light, a patterning of the direction and birefringence of the film is enabled. Reversion of the alignment direction of liquid crystal (LC) on some types of photo-cross-linkable polymer surfaces has been explored by changing exposure doses of LPUV light.<sup>6,23–26</sup> This may offer the multidomain alignment of LC materials. In these cases, the direction of interaction between the LC and polymer surfaces may be dependent on the exposure dose. The in-plane and out-of-plane switching of photoorientation of polymer films has been observed in some azobenzene-containing PLCs by adjusting exposure doses of LP light or by controlling the annealing process,<sup>16,17</sup> although the direction of the in-plane orientation is always perpendicular to  $\mathbf{E}$ . To date, no photoreactive polymer materials have been reported which can self-induce the reversion of in-plane molecular orientation.

The purpose of this paper is to develop a novel photo-cross-linkable PLC that can generate high orientational order and induce the reversion of the in-plane reorientational direction. The influence of the photoisomerization reaction on the reorientational behavior of the PLC containing the cinnamoyl group was then clarified. To this end, novel photo-cross-linkable methacrylates with a 4-methoxycinnamoyloxybiphenyl side group was synthesized, and reversion of the in-plane reorientation direction of the mesogenic groups of PLC films generated by irradiation with LPUV light and subsequent annealing was demonstrated. The orientational behavior of the film was studied using polarization UV–vis and FT-IR spectroscopies. Since the mesogenic group in this study contains a 4-methoxycinnamoyl group, in which the absorption band is separated from that of the biphenyl group, spectral analysis was performed to investigate the photoproduct influence on reorientational behavior. We have determined that the thermally

\* Corresponding author.

Scheme 1



enhanced reorientation direction is dependent on the distribution of photoproducts and the degree of photo-reaction. Furthermore, the greatest orientational order of a photo-cross-linkable PLC system has been observed.

## 2. Experimental Section

**2.1. Materials and Monomer Synthesis.** All starting materials were used as received from Tokyo Kasei Chemicals. The syntheses of methacrylate monomers (nCB) and compounds **1–3** are outlined in Scheme 1.

4-Acetoxy-4'-methoxybiphenyl (**1**) was synthesized by a conventional method from 4-methoxy-4'-hydroxybiphenyl and acetic anhydride, while methyl (E)-4-methoxycinnamate (**2**) was generated from 4-methoxycinnamoyl chloride and methanol. The syntheses of these compound were confirmed by  $^1\text{H}$  NMR and FTIR spectroscopies. The model compound 4'-methoxybiphenyl (E)-4-methoxycinnamate (**3**) was synthesized from 4-methoxycinnamoyl chloride and 4-methoxy-4'-hydroxybiphenyl in 51% yield; mp 202 °C,  $T_i > 300$  °C.  $^1\text{H}$  NMR ( $\text{CDCl}_3$ ):  $\delta$  (ppm) 3.86 (s, 6H, Ph-OCH<sub>3</sub>), 4.27 (t,  $J = 15.8$  Hz, 2H, -COO-CH<sub>2</sub>-), 4.52 (t, 2H,  $J = 4.75$  Hz, -CH<sub>2</sub>-O-Ph), 5.60 (s, 1H, CH<sub>2</sub>=C(CH<sub>3</sub>)), 6.16 (s, 1H, CH<sub>2</sub>=C(CH<sub>3</sub>)), 6.52 (d,  $J = 15.8$  Hz, 1H, -CH=CH-Ph), 6.93–6.96 (m, 2H, cinnamoyl-Ph), 6.97–6.99 (m, 4H, Ph-Ph), 7.2–7.21 (m, 2H, cinnamoyl-Ph), 7.5–7.51 (m, 4H, Ph-Ph), 7.83–7.86 (d,  $J = 15.8$  Hz, 1H, -CH=CH-Ph). IR (KBr): 2966, 1722, 1631, 1599, 1494, 1137, 830 cm<sup>-1</sup>.

4'-(4-Methoxycinnamoyl)-4-phenylphenoxyalkyl methacrylates (**2CB** and **6CB**) were synthesized from 4'-hydroxy-4-phenylphenoxyalkyl methacrylate<sup>27</sup> and 4-methoxycinnamoyl chloride according to the usual method.<sup>27</sup> Yield, mp, NMR, and IR spectroscopic characteristics are as follows: **2CB**: yield 39%, mp 145 °C.  $^1\text{H}$  NMR ( $\text{CDCl}_3$ ):  $\delta$  (ppm) 1.96 (s, 3H, CH<sub>2</sub>=C(CH<sub>3</sub>)), 3.86 (s, 3H, Ph-OCH<sub>3</sub>), 4.27 (t,  $J = 4.75$  Hz, 2H, -COO-CH<sub>2</sub>-), 4.52 (t, 2H,  $J = 4.75$  Hz, -CH<sub>2</sub>-O-Ph), 5.60 (s, 1H, CH<sub>2</sub>=C(CH<sub>3</sub>)), 6.16 (s, 1H, CH<sub>2</sub>=C(CH<sub>3</sub>)), 6.52 (d,  $J = 15.8$  Hz, 1H, -CH=CH-Ph), 6.93–6.96 (m, 2H, cinnamoyl-Ph), 6.97–6.99 (m, 4H, Ph-Ph), 7.2–7.21 (m, 2H, cinnamoyl-Ph), 7.5–7.51 (m, 4H, Ph-Ph), 7.83–7.86 (d,  $J = 15.8$  Hz, 1H, -CH=CH-Ph). IR (KBr): 2935, 1723, 1632, 1600, 1495, 1245, 1134, 826 cm<sup>-1</sup>. **6CB**: yield 38%, mp 89 °C.  $^1\text{H}$  NMR ( $\text{CDCl}_3$ ):  $\delta$  (ppm) 1.47–1.57 (m, 4H, -O-

**Table 1.** Yield, Molecular Weight, and Thermal Properties of Synthesized PLCs

	yield (%)	$M_w \times 10^{-3}$ (g/mol)	$M_w/M_n$	$T_g^c$ (°C)	$T_m$ (°C)	phase	$T_i$ (°C)
<b>P2CB</b>	60	78.6	2.9	148	153	N	>300
<b>P6CB</b>	51	67.8	3.1	105	116	N	>300

<sup>a</sup> Molecular weight of hydrolyzed polymer (main part is poly(methacrylic acid)). Determined by GPC using polystyrene standard. THF was used for eluent. <sup>b</sup> Determined by polarization optical microscopy and DSC. <sup>c</sup>  $T_g$  = glass transition,  $T_m$  = melting point,  $T_i$  = clearing point, N = nematic. Both polymer did not exhibit  $T_i$  up to 300 °C. <sup>d</sup> Both polymer did not exhibit clear glass transition. It seems that the side groups become a crystalline structure above  $T_g$ .

(CH<sub>2</sub>)<sub>2</sub>-(CH<sub>2</sub>)<sub>2</sub>-(CH<sub>2</sub>)<sub>2</sub>-O-), 1.70–1.88 (m, 4H, -O-CH<sub>2</sub>-CH<sub>2</sub>-(CH<sub>2</sub>)<sub>2</sub>-CH<sub>2</sub>-O-), 1.95 (s, 3H, CH<sub>2</sub>=C(CH<sub>3</sub>)), 3.86 (s, 3H, Ph-OCH<sub>3</sub>), 4.00 (t,  $J = 6.6$  Hz, 2H, -COO-CH<sub>2</sub>-), 4.17 (t,  $J = 6.6$  Hz, 2H, -CH<sub>2</sub>-O-Ph), 5.55 (s, 1H, CH<sub>2</sub>=C(CH<sub>3</sub>)), 6.10 (s, 1H, CH<sub>2</sub>=C(CH<sub>3</sub>)), 6.52 (d,  $J = 15.8$  Hz, 1H, -CH=CH-Ph), 6.93–6.95 (m, 4H, Ph), 6.99–7.2 (m, 2H, Ph), 7.21–7.22 (m, 2H, cinnamoyl-Ph), 7.51–7.52 (m, 2H, Ph-Ph), 7.55–7.83 (m, 2H, Ph-Ph), 7.85 (d,  $J = 15.8$  Hz, 1H, -CH=CH-Ph). IR (KBr): 2935, 1722, 1632, 1599, 1500, 1145, 829 cm<sup>-1</sup>.

**2.2. Polymerization.** The polymerization of methacrylate monomers **2CB** and **6CB** was performed utilizing a free radical solution polymerization in tetrahydrofuran (THF) with 2,2'-azobis(isobutyronitrile) (AIBN) as the initiator. The concentration of monomers and AIBN were 10% (w/v) and 2 mol %, respectively. As an example of a general polymerization procedure, the synthesis of polymer **P6CB** is given below.

**6CB** and AIBN were dissolved in THF, and the reaction mixture was treated with a gentle stream of nitrogen. After sealing, the mixture was heated to 60 °C for 24 h. The resulting homogeneous solution was added dropwise into excess amount of diethyl ether to precipitate the polymer. After two additional precipitations from a dichloromethane solution into diethyl ether, the polymer was extracted with diethyl ether for 1 day. The polymer was dried at 25 °C under vacuum for 48 h. In the case of the polymerization of **2CB**, the resultant polymer, **P2CB**, was precipitated during the polymerization because of its low solubility in THF at 60 °C. Table 1 summarizes the yield, molecular weight, and thermal properties of synthesized PLCs. NMR and IR spectroscopic characteristics of **P2CB** and **P6CB** are as follows:

**P2CB**:  $^1\text{H}$  NMR ( $\text{CDCl}_3$ /hexafluoro-2-propanol = 1/1):  $\delta$  (ppm) 1.0 (brs, 3H, CH<sub>2</sub>-C(CH<sub>3</sub>)), 1.26 (brs, 2H, CH<sub>2</sub>-C(CH<sub>3</sub>)), 4.12 (m, 2H, -COO-CH<sub>2</sub>-), 4.50–4.51 (m, 2H, -CH<sub>2</sub>-O-Ph), 6.37 (m, 1H, -CH=CH-Ph), 6.85–6.97 (m, 6H, Ph), 7.26–7.39 (m, 6H, Ph-Ph), 7.74 (m, 1H, -CH=CH-Ph). Signal of Ph-OCH<sub>3</sub> group is overlapped with the solvent. IR (KBr): 2930, 1723, 1632, 1600, 1495, 1245, 1134, 826 cm<sup>-1</sup>. **P6CB**:  $^1\text{H}$  NMR ( $\text{CDCl}_3$ ):  $\delta$  (ppm) 1.47–1.57 (m, 6H, -O-(CH<sub>2</sub>)<sub>2</sub>-(CH<sub>2</sub>)<sub>2</sub>-(CH<sub>2</sub>)<sub>2</sub>-O- and CH<sub>2</sub>-C(CH<sub>3</sub>)), 1.70–1.88 (m, 4H, -O-CH<sub>2</sub>-CH<sub>2</sub>-(CH<sub>2</sub>)<sub>2</sub>-CH<sub>2</sub>-O-), 1.74 (s, 3H, CH<sub>2</sub>=C(CH<sub>3</sub>)), 3.51 (s, 3H, Ph-OCH<sub>3</sub>), 3.64 (t,  $J = 6.6$  Hz, 2H, -COO-CH<sub>2</sub>-), 3.81 (t,  $J = 6.6$  Hz, 2H, -CH<sub>2</sub>-O-Ph), 6.41 (d,  $J = 15.8$  Hz, 1H, -CH=CH-Ph), 6.93–6.96 (m, 2H, Ph), 7.0–7.2 (m, 4H, Ph), 7.42–7.49 (m, 4H, cinnamoyl-Ph), 7.51–7.52 (m, 2H, Ph), 7.85 (d,  $J = 15.8$  Hz, 1H, -CH=CH-Ph). IR (KBr): 2930, 1723, 1632, 1599, 1495, 1245, 1145, 829 cm<sup>-1</sup>.

**2.3. Characterization.**  $^1\text{H}$  NMR spectra were measured with Bruker DRX-500 FT-NMR apparatus. As the synthesized polymers were hardly soluble in THF at room temperature, they were hydrolyzed before molecular weight determination by gel permeation chromatography (GPC). The hydrolysis was carried out by refluxing the polymers in 10/80/10 wt/wt/wt % sodium hydroxide/THF/water solution for 2 days, resulting in a soluble polymer in THF. By the  $^1\text{H}$  NMR analysis, the main part of the hydrolyzed polymer was poly(methacrylic acid), although further identification was not carried out at present.

**Table 2. Spectral Analysis of Model Compound 3**

wavelength (nm)	absorption coefficients ( $\epsilon$ ) <sup>a</sup>		
	<i>E</i> -isomer	<i>Z</i> -isomer	<i>PF</i> -Product
315	$3.65 \times 10^4$	$1.90 \times 10^4$	$0.16 \times 10^4$
330	$2.57 \times 10^4$	$1.53 \times 10^4$	$0.55 \times 10^4$
365	0	0	$1.11 \times 10^4$

<sup>a</sup> Absorption coefficients ( $\text{L mol}^{-1} \text{cm}^{-1}$ ) in methylene chloride solution.

The molecular weight of these hydrolyzed polymers was measured by GPC (Tosoh HLC-8020 GPC system with Tosoh TSKgel column; eluent, THF) calibrated using polystyrene standards. Thermal properties were examined using a polarization optical microscope (Olympus BHA-P) equipped with a Linkam TH600PM heating and cooling stage in addition to differential scanning calorimetry (DSC; Seiko-I SSC5200H) analysis at a heating and cooling rate of 10 K/min. Polarization FTIR spectra were recorded through a JASCO FTIR-410 system with an attached wire-grid polarizer. Polarization UV-vis spectra were measured using a Hitachi U-3030 spectrometer equipped with Glan-Taylor polarizing prisms. The in-plane order parameter,  $S$ , is expressed in the form of eq 1:<sup>23</sup>

$$S = \frac{A_p - A_s}{A_{(\text{large})} + 2A_{(\text{small})}} \quad (1)$$

where  $A_p$  and  $A_s$  are the absorbances parallel and perpendicular to **E**, respectively, while  $A_{(\text{large})}$  is taken to be the larger of  $A_p$  and  $A_s$ , while  $A_{(\text{small})}$  is taken to be the smaller.  $S$  was calculated by polarized UV-vis spectroscopy at a wavelength of 320 nm.

**2.4. Photoirradiation.** Thin films of **PnCB** were prepared by spin-coating a methylene chloride solution or a hexafluoro-2-propanol (6FP) solution of polymers (~5 wt %) onto a quartz or CaF<sub>2</sub> substrate. The film thickness was 0.2–0.5  $\mu\text{m}$ , which was determined by the stylus contact method using Taly-Step (Rank Taylor Hobson). The film was set on a Linkam TH600PM heating stage and irradiated by light from a 250 W high-pressure Hg-UV lamp which passed through Glan-Taylor polarizing prisms with a cutoff filter under 290 nm. The light intensity was about 50 mW/cm<sup>2</sup> at 313 nm. The optical anisotropy of the film was measured by polarizing microscopy and polarization UV-vis and FT-IR spectra.

**2.5. Spectral Analysis.** Thin films of **PnCB**s were irradiated with UV light, and the absorption spectra were measured at intervals. The molar extinction coefficient of the *Z*-isomer and photo-Friez (*PF*) product of **3** at each wavelength were calculated using the determination of the *E/Z* and *E/PF* ratios by means of HPLC analysis. Table 2 summarizes the results. Spectral analysis of **PnCB** was performed using the procedure given by Ichimura et al.<sup>28</sup> according to the following expression:

$$D_{315\text{nm}} = \epsilon_{E(315\text{nm})}[E] + \epsilon_{Z(315\text{nm})}[Z] + \epsilon_{PF(315\text{nm})}[PF]$$

$$D_{330\text{nm}} = \epsilon_{E(330\text{nm})}[E] + \epsilon_{Z(330\text{nm})}[Z] + \epsilon_{PF(330\text{nm})}[PF]$$

$$D_{365\text{nm}} = \epsilon_{E(365\text{nm})}[E] + \epsilon_{Z(365\text{nm})}[Z] + \epsilon_{PF(365\text{nm})}[PF]$$

where  $D_{315\text{nm}}$ ,  $D_{330\text{nm}}$ , and  $D_{365\text{nm}}$  are the absorbances during photolysis,  $\epsilon_{E(315\text{nm})}$ ,  $\epsilon_{Z(315\text{nm})}$ , and  $\epsilon_{PF(315\text{nm})}$  are the absorbance coefficients of *E*-isomer, *Z*-isomer, and photo-Friez products at the corresponding wavelength, and  $[E]$ ,  $[Z]$ , and  $[PF]$  are their concentrations.

### 3. Results and Discussion

**3.1. Photochemistry of PnCB Films.** The synthesized PLCs exhibit a nematic liquid crystalline phase as summarized in Table 1. Both polymers are insoluble in THF at room temperature, while **P6CB** is soluble in chloroform, methylene chloride, and dimethylformamide. However, **P2CB** is insoluble in such solvents and only soluble in 6FP. Therefore, thin films were prepared

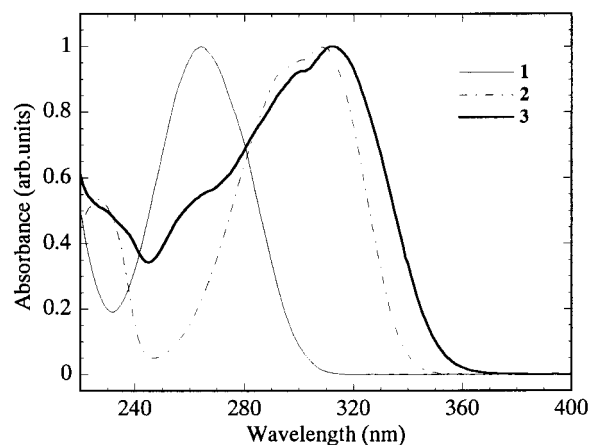


**Figure 1.** UV absorption spectrum of model compounds **1–3** in a methylene chloride solution.

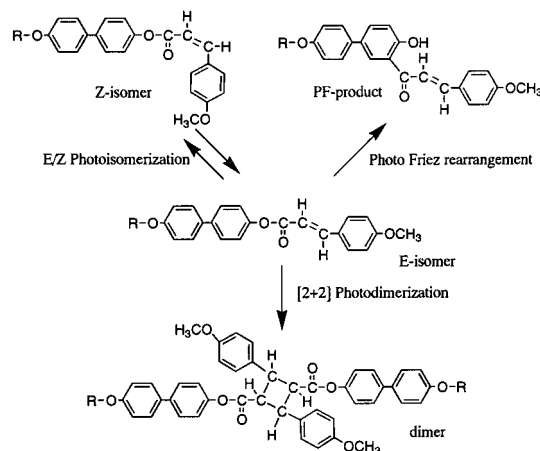


**Figure 2.** Possible types of photoreaction of the mesogenic group of 4-methoxycinnamoyloxybiphenyl.

by the spin-coating method from a methylene chloride solution for **P6CB** and from a 6FP solution for **P2CB**.

To analyze the photoreaction of **PnCB** films, we initially examined the UV spectra of model compounds **1–3** in methylene chloride solution as shown in Figure 1. Model compound **3** has a mesogenic side group identical to that of **PnCB**, and the spectrum is similar to that of **P6CB**. It reveals that **3** exhibits several absorption peaks that could be considered as the absorption bands for **1** and **2**. Since absorption of **2** longer than 305 nm does not overlap with that of **1**, the absorption of the cinnamate group in **3** could approximately be separated from the absorption of the biphenyl group. This may allow evaluation of the photoreaction of the cinnamate group of **3** using absorption bands longer than 305 nm.

It is well-known that irradiation of phenyl cinnamate derivatives with UV light produces three types of photoproducts as shown in Figure 2, i.e., a photodimerized product (photodimer), a photoisomerized product (*Z*-isomer), and a product from photo-Friez (*PF*) rearrangement.<sup>27,29</sup> Figure 3 illustrates the spectral change of **P6CB** film upon a quartz substrate. Film absorption was found to decrease monotonically, exhibiting a slight increase at longer wavelengths. This increase in the absorption at longer wavelengths is attributed to formation of a very small amount of *PF* product. The suppression of the photo-Friez rearrangement reaction in the film state is reported when using a methacrylate polymer with 4-cinnamoyloxybiphenyl side groups.<sup>27</sup>



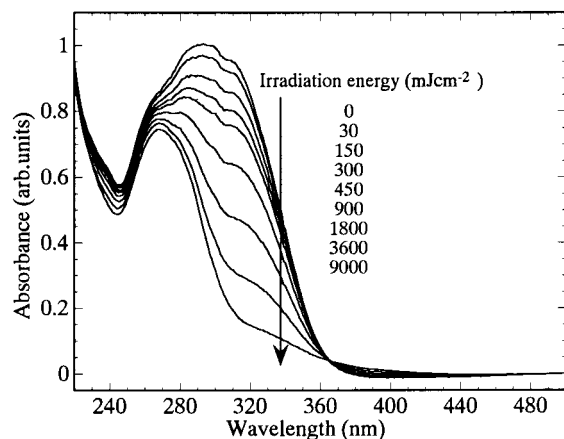


**Figure 3.** UV absorption spectral changes in **P6CB** film during the course of irradiation with UV light.

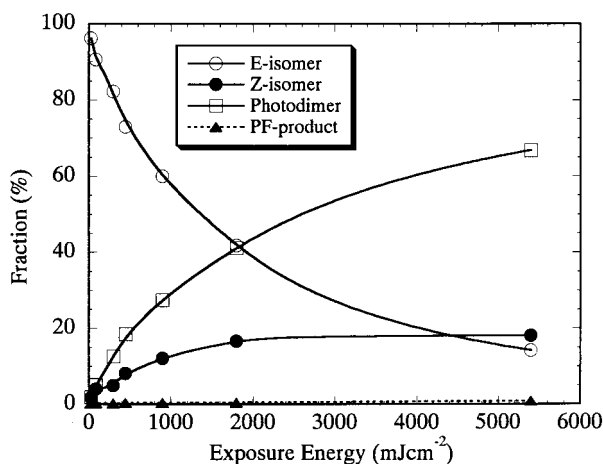


**Figure 4.** Fractions of *E*- (○) and *Z*- (●) isomers, photodimers (□), and photo-Fries products (▲) in thin films of **P6CB** as a function of exposure energy.

Therefore, the major photoproducts will come from photodimerization and photoisomerization reactions of the mesogenic group.

Spectral analysis was performed according to Ichimura's method using spectral parameters as listed in Table 2.<sup>28</sup> Results for the **P6CB** film plotted in Figure 4 reveal both photodimerization and photoisomerization take place at an early stage of photoirradiation, although the amount of the photodimer produced is larger than that of the *Z*-isomer. Additionally, the amount of *Z*-isomer produced was found to have an upper limit of 18–20% over a prolonged exposure. The formation of *PF* products amounts to less than 1% over all exposure doses. Similar results were obtained for **P2CB** films. A greater degree of photodimerization relative to photoisomerization had been reported for methacrylates with cinnamate side group having a para substituent.<sup>28</sup>

**3.2. Enhancement and Reversion of Photoinduced Optical Anisotropy.** Irradiation of a polymer containing cinnamoyl groups with LPUV light leads to negative optical anisotropy as a result of axis-selective [2 + 2] photodimerization as well as *E*-to-*Z* photoisomerization.<sup>5,6,23,28,30</sup> If a polymer with cinnamoyl groups exhibits a liquid crystalline phase, the photoinduced optical anisotropy generated in an amorphous state of the as-coated polymer film may change when the film is annealed at elevated temperatures owing to its liquid crystalline nature.<sup>5,20–23</sup> Accordingly, for **PnCB**, irradiation with LPUV light generates a small

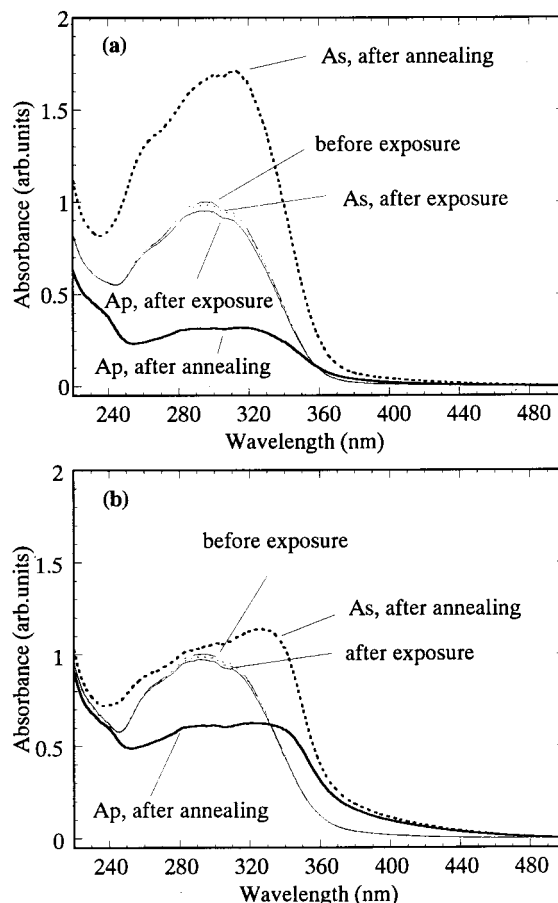


**Figure 5.** UV polarization spectrum of **PnCB** films before photoirradiation, after irradiation with 30 mJ cm<sup>-2</sup> doses (thin lines), and after subsequent annealing (thick lines). *A<sub>p</sub>* is shown as the solid lines, and *A<sub>s</sub>* is shown as the dotted lines. (a) **P2CB** film, annealed at 170 °C for 1 min; (b) **P6CB** film, annealed at 130 °C for 1 min.

negative  $\Delta A$ , and subsequent annealing will yield pronounced adjustment of spectral intensities.

Figure 5a shows polarized UV-vis spectral differences between a **P2CB** film irradiated with 30 mJ cm<sup>-2</sup> doses of LPUV light and that film following subsequent annealing at 160 °C for 5 min. After exposure, a small negative  $\Delta A$  is generated as annealing induces enhancement of the negative anisotropy. The enhanced reorientation direction of mesogenic groups is perpendicular to **E** of LPUV light, and the orientational order parameter *S* is amplified from -0.009 to -0.61. The thermal enhancement of negative  $\Delta A$  is also observed for PLCs with azobenzene side groups, where separate mechanisms have been elucidated with respect to *E*-to-*Z* photoisomerization and thermal reorientation.<sup>7–15</sup> The first mechanism was clarified through use of an LP light at a wavelength of 436 nm, where the major component of the rod-shaped *E*-isomer of azobenzene resides in a direction perpendicular to **E** and amplifies the negative  $\Delta A$ .<sup>14</sup> The second mechanism involves the generation of considerable amounts of the *Z*-isomer in a direction parallel to **E** by the use of 365 nm LPUV light which lowers the phase transition temperature by accelerating thermal motion of the azobenzene side groups.<sup>15</sup> In the case of **P2CB** irradiated with 30 mJ cm<sup>-2</sup> doses, the photogenerated *Z*-isomer and the photodimer are 1.5% and 1.9%, respectively. Reorientation of the mesogenic groups during photoirradiation will scarcely occur as the mobility of the mesogenic groups at room temperature

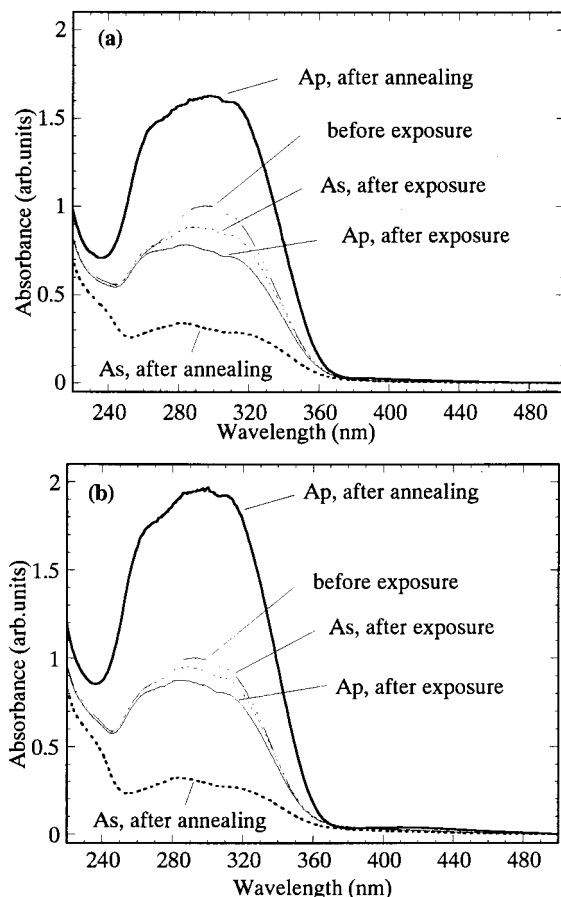


**Figure 6.** UV polarization spectrum of **P<sub>n</sub>CB** films before photoirradiation, after irradiation with  $450 \text{ mJ cm}^{-2}$  doses (thin lines), and after subsequent annealing (thick lines).  $A_p$  is shown as the solid lines, and  $A_s$  is shown as the dotted lines. (a) **P2CB** film, annealed at  $180^\circ\text{C}$  for 1 min. (b) **P6CB** film, annealed at  $155^\circ\text{C}$  for 1 min.

is quite low while the photoinduced  $\Delta A$  is very small. Therefore, thermal enhancement of negative  $\Delta A$  will be triggered by a small amount of *Z*-isomer and photo-cross-linked photodimer in a direction parallel to **E**, which may lower the  $T_m$  of the film analogously to the behavior of the polymer with azobenzene groups.<sup>15</sup> A detailed discussion is provided in section 3.5. In addition, the thermal enhancement of negative  $\Delta A$  is also observed for films of **P6CB**, although a red shift of the absorption band takes place, as shown in Figure 5b. This red shift is a consequence of the *J*-aggregation of mesogenic groups caused by annealing and results in a lower  $\Delta A$  in comparison with that of **P2CB**.

In contrast, reversion of the amplification of the thermal reorientation order is observed when the irradiation dose is  $450 \text{ mJ cm}^{-2}$ , as shown in Figure 6. In these cases, the amounts of photogenerated *Z*-isomer and photodimer are 7% and 17% for **P2CB** and 8% and 17% for **P6CB**, respectively. This shows that the photoinduced negative optical anisotropy after exposure is larger than in films with  $30 \text{ mJ cm}^{-2}$  doses because of the larger degree of axis-selective photoreaction. This strongly suggests that an efficient, axis-selective, photo-cross-linking reaction of the cinnamoyl group is occurring. After annealing, *S* is amplified from  $-0.05$  to  $+0.60$  for **P2CB** and from  $-0.03$  to  $+0.68$  for **P6CB**. This phenomenon is attributed to the thermally enhanced reorientation of unreacted mesogenic groups along the photo-cross-linked mesogenic groups in a direction

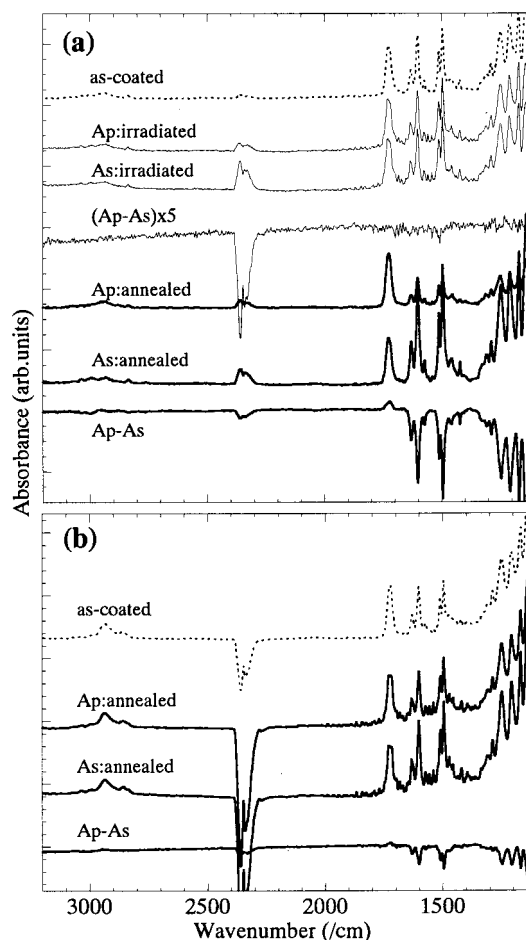


**Figure 7.** FT-IR spectra of **P<sub>n</sub>CB** films on  $\text{CaF}_2$  substrates before photoirradiation (dotted lines), after irradiation with  $30 \text{ mJ cm}^{-2}$  doses (thin lines), and after subsequent annealing (thick lines). (a) **P2CB** film, annealed at  $170^\circ\text{C}$  for 1 min. (b) **P6CB** film, annealed at  $130^\circ\text{C}$  for 1 min.

parallel to **E**. The axis-selective irradiation decreases mobility of the photo-cross-linked mesogenic groups that can control the reorientational direction as reported previously,<sup>20–22</sup> while the greatest values of enhanced order parameters are obtained to date for photo-cross-linkable PLC films. The thermally enhanced optical anisotropy of **P2CB** is revealed to be smaller than that of **P6CB** in Figure 6. The mobility of mesogenic groups during thermal reorientation with a shorter methylene spacer will be limited. Additionally, aggregation is suppressed for **P6CB** as a certain amount of photoreaction products will restrain molecular aggregation as a result of the decrease in liquid crystallinity of the PLC.

**3.3. FT-IR Spectroscopy.** The reversion of reorientation direction was further investigated by polarized FT-IR spectroscopy measurements. Parts a and b of Figure 7 show FT-IR spectral differences of **P2CB** and **P6CB** films prior to irradiation with LPUV light and after irradiation with  $30 \text{ mJ cm}^{-2}$  doses and subsequent annealing. After irradiation, a slight decrease in the absorption of the cinnamoyl group at  $1632 \text{ cm}^{-1}$  ( $\nu\text{C}=\text{C}$ ) is observed for **P2CB**, although differential spectra ( $A_p - A_s$ ) reveal a very small dichroism, indicating that reorientation of the mesogenic groups can be negligible. A similar change is observed for **P6CB**. Large adjustment in absorbance appeared after annealing. For **P2CB** film, intensities of absorption bands at  $1632 \text{ cm}^{-1}$ ,  $1600 \text{ cm}^{-1}$  ( $\nu\text{Ph}-\text{Ph}$ ),  $1495 \text{ cm}^{-1}$  ( $\nu\text{Ph}$ ), and  $1245$

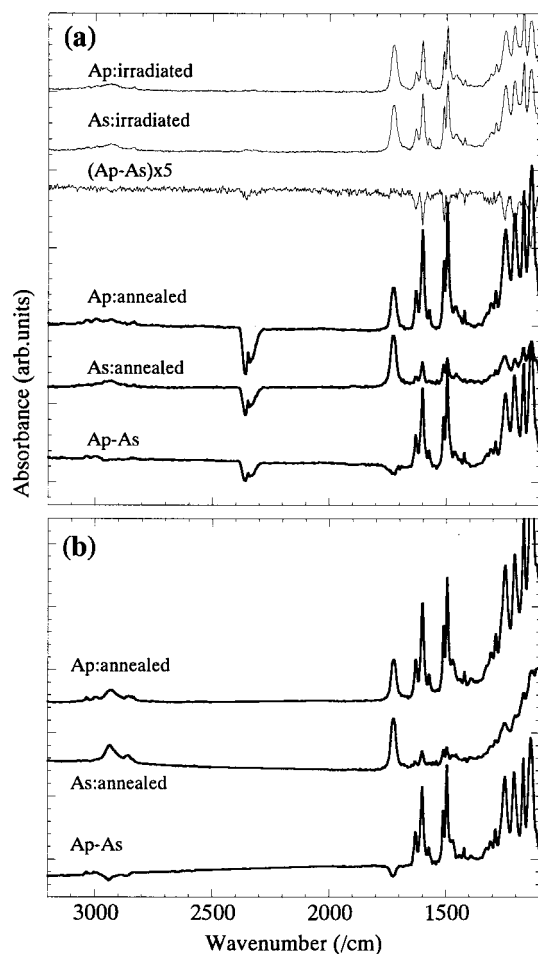


**Figure 8.** FT-IR spectra of PnCB films on  $\text{CaF}_2$  substrates after irradiation with  $450 \text{ mJ cm}^{-2}$  doses (thin lines), and after subsequent annealing (thick lines). (a) **P2CB** film annealed at  $180^\circ\text{C}$  for 1 min. (b) **P6CB** film annealed at  $155^\circ\text{C}$  for 1 min.

$\text{cm}^{-1}$  ( $\nu\text{Ph-O}$ ) are pronouncedly decreased, while a slight increase at  $1723 \text{ cm}^{-1}$  ( $\nu\text{C=O}$ ) and around  $2930 \text{ cm}^{-1}$  ( $\nu\text{C-H}$ ) can be observed.  $A_s$  absorption bands, however, exhibit opposite changes. The differential spectrum reveals clear enhancement of photoinduced dichroism in the same direction by annealing. This result indicates that mesogenic side groups thermally reorient in a direction perpendicular to **E**.  $S$  is amplified at  $1495 \text{ cm}^{-1}$  to  $-0.61$ , in good agreement with the value obtained by UV-vis spectra. For **P6CB** films, a similar tendency for adjustment in the absorption bands is observed, but the difference between  $A_p$  and  $A_s$  after annealing was found to be relatively small. This is a consequence of the aggregation of mesogenic groups as described in the above section.

When films are irradiated with  $450 \text{ mJ cm}^{-2}$  doses, there is a greater photoinduced dichroism than arises from  $30 \text{ mJ cm}^{-2}$  doses as shown in Figure 8a. In contrast to Figure 7, annealing leads to increases in absorption bands at  $1632 \text{ cm}^{-1}$ ,  $1600$ ,  $1495$ , and  $1245 \text{ cm}^{-1}$ , with decreases observed at  $1723 \text{ cm}^{-1}$  for  $A_p$  of both PLC films.  $A_s$ , however, exhibits opposite adjustment to these absorption bands. The differential spectrum reveals these changes are entirely in the opposite direction as compared to films with  $30 \text{ mJ cm}^{-2}$  doses. In addition, absorption around  $2930 \text{ cm}^{-1}$  ( $\nu\text{C-H}$ ) in the differential spectrum in Figure 8b distinctly displays negative dichroism. These results suggest that me-

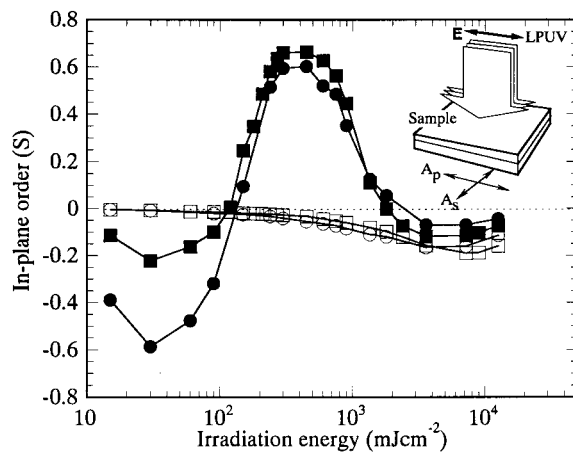


**Figure 9.** Difference in the order parameters  $S$  of **PnCB** films after irradiation with LPUV light (open points) and after subsequent annealing (closed points), as a function of the exposure energy. **P2CB** films were annealed at  $180^\circ\text{C}$  for 1 min and **P6CB** films were annealed at  $155^\circ\text{C}$  for 1 min for all cases. Circles and squares denote  $S$  for films of **P2CB** and **P6CB**, respectively.

sogenic groups including methylene spacers reorient thermally in a direction parallel to **E**. Furthermore,  $S$  values at  $1495 \text{ cm}^{-1}$  are  $+0.53$  for **P2CB** and  $+0.65$  for **P6CB**. These values are also in good agreement with that obtained by UV-vis spectra.

**3.4. Effect of Exposure Energy.** To elucidate the effect of exposure energy on the reversion of direction for thermally enhanced reorientation of mesogenic groups, films were irradiated with LPUV light over various exposure doses. Results are shown in Figure 9 where a plot of the order parameter  $S$  after irradiation and after subsequent annealing as a function of exposure energy is given. All irradiated films of **P2CB** and **P6CB** were annealed at  $180$  and  $155^\circ\text{C}$  for 1 min, respectively.

Figure 9 reveals the  $S$  value after irradiation is negative regardless of exposure dose and that increasing exposure doses for both PLCs results in increasing  $S$  values. This is due to the axis-selective photoreaction of the cinnamoyl group as described in section 3.2. When the exposure doses were less than  $100 \text{ mJ cm}^{-2}$ , annealing amplified the negative value of  $S$ , with a degree of photo-cross-linking of the side groups being less than about 13% and with the amount of *Z*-isomer being less than about 5%. Further irradiation inverts the reorientation direction after annealing. The maximum positive  $S$  is obtained when the degree of photo-cross-linking of the side groups was 15–20%, and the amount of *Z*-isomer was 7–10%. In addition, annealing of the films irradiated with doses of  $2 \text{ J cm}^{-2}$  scarcely enhanced molecular reorientation as a high degree of photo-cross-linking restricts mobilization of the mesogenic groups at elevated temperatures. These results suggest that the thermally enhanced reorientation behavior is strongly dependent on the degree of photoreaction and on the ratio of the type of photoreacted products, which may affect the thermal property of exposed film.

**3.5. Effect of Annealing Temperature.** As described above, thermally enhanced molecular reorientation is triggered by the photoinduced optical anisotropy of the irradiated film. Therefore, mobility of the mesogenic side groups will depend on the annealing temperature. Accordingly, we evaluated the reorientational behavior of films annealed at various tempera-

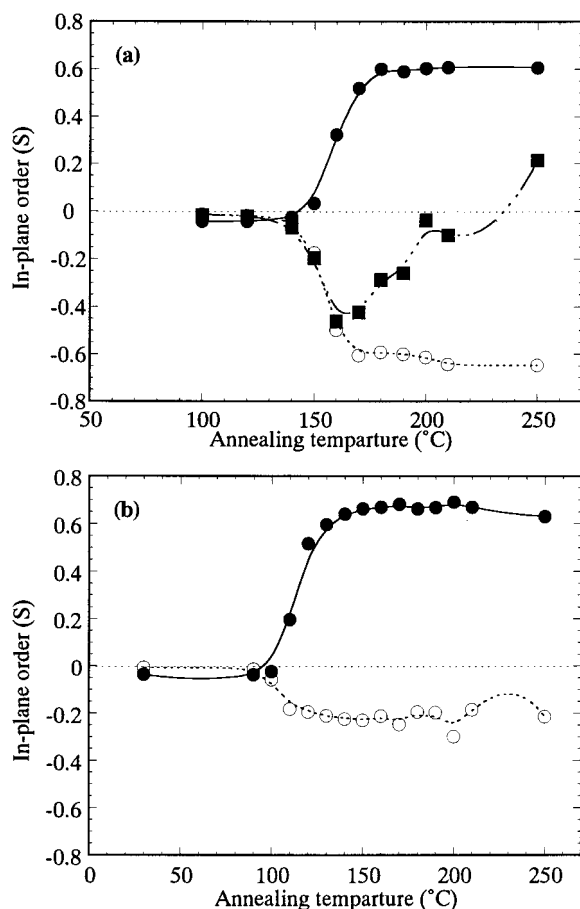


**Figure 10.** Change in in-plane order parameters ( $S$ ) of **PnCB** film as a function of annealing temperature at various irradiation doses:  $\circ$ ,  $30 \text{ mJ cm}^{-2}$ ;  $\bullet$ ,  $450 \text{ mJ cm}^{-2}$ ;  $\blacksquare$ ,  $90 \text{ mJ cm}^{-2}$ . (a) **P2CB**; (b) **P6CB**.

**Table 3. Ratio of Order Parameter  $S$  at Various Annealing Temperatures**

	doses <sup>b</sup> ( $\text{mJ cm}^{-2}$ )	$S_x/S(T_m + 35)^a$		
		$T_m - 5^\circ\text{C}$	$T_m$	$T_m + 5^\circ\text{C}$
<b>P2CB</b>	30	0.71	1.0	1.01
	450	0.25	0.53	0.65
<b>P6CB</b>	30	0.70	0.81	0.82
	450	0.27	0.42	0.76

<sup>a</sup> Ratio of order parameter annealed at  $T_x$  °C and at  $T_m + 35$  °C. <sup>b</sup> Irradiation energy. <sup>c</sup> Annealing temperature, °C.

tures, using doses of 30, 90, and  $450 \text{ mJ cm}^{-2}$ . Results shown in parts a and b of Figure 10 plot the order parameter  $S$  for both films as a function of the annealing temperature. For all cases, an explicit magnification of  $S$  appears when the annealing temperature is larger than  $T_m$  of the PLC. When films are annealed above  $T_m$ , the direction of reorientation is found to be perpendicular to **E** when irradiated with  $30 \text{ mJ cm}^{-2}$  or parallel for films subjected to  $450 \text{ mJ cm}^{-2}$  doses, respectively.  $S$  of **P2CB** films with  $90 \text{ mJ cm}^{-2}$  doses, however, are initially negatively enhanced and then positively increase upon increase of annealing temperature.

Looking closely at Figure 10, the threshold temperature for thermal reorientation varies with exposure energy. Table 3 summarizes the ratio of the thermally enhanced order parameter ( $R = S_x/S(T_m + 35)$ ) with different exposure doses, where  $S(T_m + 35)$  is taken as  $S$  at  $T_m + 35$  (°C), and  $S_x$  is  $S$  annealed at  $T_m - 5$ ,  $T_m$ , and  $T_m + 5$  (°C) of the PLCs. For both PLCs irradiated with

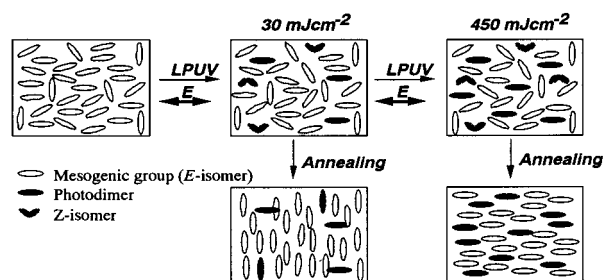


**Figure 11.** Model illustration of the reversion of thermally enhanced in-plane reorientation of **PnCB** films.

$30 \text{ mJ cm}^{-2}$  doses,  $R$  values annealed at  $T_m - 5$  are close to that at  $T_m$  and at  $T_m + 5$ . This shows that thermally enhanced reorientation occurs below  $T_m$  of the PLC when the irradiation energy is  $30 \text{ mJ cm}^{-2}$ , indicating  $T_m$  of the PLC decreased after exposure as described in section 3.2. In contrast,  $R$  values for PLC irradiated with  $450 \text{ mJ cm}^{-2}$  doses gradually increase with increasing annealing temperature, and  $R$  values at  $T_m - 5$  are much less than for films with  $30 \text{ mJ cm}^{-2}$  doses. It is suggested that the larger amount of photo-cross-linked side groups restrict the mobility of mesogenic side groups rather than lowering the  $T_m$  of the film; i.e., photo-cross-linked side groups control the thermally enhanced molecular reorientation in a direction parallel to **E**.

For **P2CB** film irradiated for  $90 \text{ mJ cm}^{-2}$ , it is interesting that the enhanced negative value of  $S$  decreased with increasing annealing temperature and became positive with an annealing temperature of  $250^\circ\text{C}$ . This indicates reorientation in a direction perpendicular to **E** is generated by a similar manner with film irradiated at  $30 \text{ mJ cm}^{-2}$  when an annealing temperature of about  $T_m$  is used. However, nonmobile photo-cross-linked groups could act as the command group for thermal reorientation in a direction parallel to **E** when the annealing temperature is increased.

#### 4. Conclusions

The reversion of in-plane reorientation of PLC films was investigated by irradiation with linearly polarized ultraviolet (LPUV) light and subsequent annealing, whereby a high orientational order in both directions was achieved. Spectral analysis of the films suggested that both photoisomerization reactions and the photo-cross-linking reactions occurred in the mesogenic groups of the films, with the degree of the photo-cross-linking reaction occurring to a greater extent than that of others and with the photo-Fries rearrangement occurring to the least extent. The mechanism of reversion of the orientational direction can be related to the degree and type of photoreaction of the mesogenic groups, as illustrated in Figure 11. Thermal amplification of the perpendicular orientation of the films is induced by a small amount of photoproducts in a direction parallel to **E**, resulting in reorientation of the mesogenic groups perpendicular to **E**. On the other hand, when the degree of the photo-cross-linking becomes sufficient in a direction parallel to **E**, reversion of orientation direction is generated because of the decrease in mobility at an elevated temperature in a direction parallel to **E**. We anticipate these photoreactive PLC films may find application in new optical devices such as birefringent films for LCD and in optical memory devices.



**Acknowledgment.** This work was supported by a Grant-in-aid for Scientific Research from the Ministry of Education, Science and Culture of Japan.

## References and Notes

- (1) Shibaev, V. P.; Kostromin, S. G.; Ivanov, S. A. *Polymers as Electroactive and Photooptical Media*; Shibaev, V. P., Ed.; Springer: Berlin, 1996; p 37.
- (2) (a) MacArdle, C. B. *Applied Photochromic Polymer Systems*; MacArdle, C. B., Ed.; Blackie: New York, 1991; p 1. (b) Krongauz, V. *Applied Photochromic Polymer Systems*; MacArdle, C. B., Ed.; Blackie: New York, 1991; p 121.
- (3) Anderle, K.; Birenheide, R.; Eich, M.; Wendrorff, J. H. *Makromol. Chem. Rapid Commun.* **1989**, *10*, 477.
- (4) Benecke, C.; Seiberle, H.; Schadt, M. *Jpn. J. Appl. Phys.* **2000**, *39*, 525.
- (5) Ichimura, K. *Chem. Rev.* **2000**, *100*, 1847.
- (6) O'Neil, M.; Kelly, S. M. *J. Phys. D: Appl. Phys.* **2000**, *33*, R67.
- (7) (a) Fischer, T.; Läsker, L.; Stumpe, J. *J. Photochem. Photobiol. A: Chem.* **1994**, *80*, 453. (b) Andrews, S. R.; Williams, G.; Läsker, L.; Stumpe, J. *Macromolecules* **1995**, *28*, 8863. (c) Fischer, T.; Läsker, L.; Czaplá, S.; Rübner, J.; Stumpe, J. *Mol. Cryst. Liq. Cryst.* **1997**, *298*, 213.
- (8) (a) Holme, N. C. R.; Ramanujam, P. S.; Hvilsted, S. *Appl. Opt.* **1996**, *35*, 4622. (b) Ramanujam, P. S.; Holme, C.; Hvilsted, S.; Pedersen, M.; Andruzzi, F.; Paci, M.; Tassi, E.; Magagnini, P.; Hoffman, U.; Zebger, I.; Siesler, H. W. *Polym. Adv. Technol.* **1996**, *7*, 768.
- (9) (a) Wu, Y.; Zhang, Q.; Kanazawa, A.; Shiono, T.; Ikeda, T. *Macromolecules* **1999**, *32*, 3951. (b) Wu, Y.; Demachi, Y.; Tsutsumi, O.; Kanazawa, A.; Shiono, T.; Ikeda, T. *Macromolecules* **1998**, *31*, 4457. (c) Wu, Y.; Demachi, Y.; Tsutsumi, O.; Kanazawa, A.; Shiono, T.; Ikeda, T. *Macromolecules* **1998**, *31*, 1104. (d) Wu, Y.; Demachi, Y.; Tsutsumi, O.; Kanazawa, A.; Shiono, T.; Ikeda, T. *Macromolecules* **1998**, *31*, 349.
- (10) Meng, X.; Natansohn, A.; Rochon, P. *Supramol. Sci.* **1996**, *3*, 207.
- (11) Labarthe, F.; Freiberg, S.; Pellerin, C.; Pézolet, M.; Natansohn, A.; Rochon, P. *Macromolecules* **2000**, *33*, 6815.
- (12) Ruslim, C.; Ichimura, K. *Macromolecules* **1999**, *32*, 4254.
- (13) Han, M.; Morino, S.; Ichimura, K. *Chem. Lett.* **1999**, 645.
- (14) Han, M.; Ichimura, K. *Macromolecules* **2001**, *34*, 82.
- (15) Han, M.; Ichimura, K. *Macromolecules* **2001**, *34*, 90.
- (16) Han, M.; Morino, S.; Ichimura, K. *Macromolecules* **2000**, *33*, 6360.
- (17) (a) Meier, J. G.; Ruhmann, R.; Stumpe, J. *Macromolecules* **2000**, *33*, 843. (b) Stumpe, J.; Fischer, T.; Rutloh, M.; Meier, J. G. *Proc. SPIE* **1999**, *3800*, 150.
- (18) Kidowaki, M.; Fujiwara, T.; Morino, S.; Ichimura, K.; Stumpe, J. *Appl. Phys. Lett.* **2000**, *76*, 1377.
- (19) Date, R. W.; Fawcett, A. H.; Geue, T.; Haferkorn, J.; Malcolm, R. K.; Stumpe, J. *Macromolecules* **1998**, *31*, 4935.
- (20) Kawatsuki, N.; Takatsuka, H.; Yamamoto, T.; Sengen, O. *J. Polym. Sci., Part A: Polym. Chem.* **1998**, *36*, 1521.
- (21) (a) Kawatsuki, N.; Suehiro, C.; Yamamoto, T. *Macromolecules* **1998**, *31*, 5984. (b) Kawatsuki, N.; Matsuyoshi, K.; Yamamoto, T. *Macromolecules* **2000**, *33*, 1698.
- (22) (a) Kawatsuki, N.; Suehiro, C.; Shindo, H.; Yamamoto, T.; Ono, H. *Macromol. Rapid Commun.* **1998**, *19*, 201. (b) Kawatsuki, N.; Yamamoto, T.; Ono, H. *Appl. Phys. Lett.* **1999**, *74*, 935.
- (23) (a) Kawatsuki, N.; Ono, H.; Takatsuka, H.; Yamamoto, T.; Sengen, O. *Macromolecules* **1997**, *30*, 6680. (b) Kawatsuki, N.; Takatsuka, H.; Yamamoto, T.; Ono, H. *Jpn. J. Appl. Phys.* **1997**, *36*, 6469.
- (24) Obi, M.; Morino, S.; Ichimura, K. *Jpn. J. Appl. Phys.* **1999**, *38*, L145.
- (25) (a) Obi, M.; Morino, S.; Ichimura, K. *Macromol. Rapid Commun.* **1998**, *19*, 643. (b) Obi, M.; Morino, S.; Ichimura, K. *Chem. Mater.* **1999**, *11*, 656.
- (26) Kawatsuki, N.; Matsuyoshi, K.; Hayashi, M.; Takatsuka, H.; Yamamoto, T. *Chem. Mater.* **2000**, *12*, 1549.
- (27) Kawatsuki, N.; Sakashita, S.; Takatani, K.; Yamamoto, T.; Sengen, O. *Macromol. Chem. Phys.* **1996**, *197*, 1919.
- (28) Ichimura, K.; Akita, Y.; Akiyama, H.; Kudo, K.; Hayashi, Y. *Macromolecules* **1997**, *30*, 903.
- (29) Turro, N. J. *Modern Molecular Photochemistry*; The Benjamin/Cummings Publishing: Menlo Park, 1978.
- (30) Schadt, M.; Schmitt, K.; Kozinkov, V.; Chigrinov, V. *Jpn. J. Appl. Phys.* **1992**, *34*, 2155.

MA011439U